



Report For Fluidization XVI

A modified model for predicting bed density of air dense medium gas-solid fluidized bed (ADMGFB) using binary dense media

Name : Chengguo LIU

Department: China University of Mining and Technology

E-mail: chengguo_liu@cumt.edu.cn

May 28, 2019 Guilin China



Outlines

1. Introduction
2. Experimental
3. Result and discussion
4. Conclusion

➤ Necessity of dry coal preparation

- ❑ Since 1980s, the separation rate of raw coal in China has increased from 18.4% to 71.8%, but there is still a big gap from the developed countries in the world.
- ❑ More than 2/3 raw coal in China is distributed in arid and water-scarce areas in Western China, so it is difficult to adopt wet separation method.

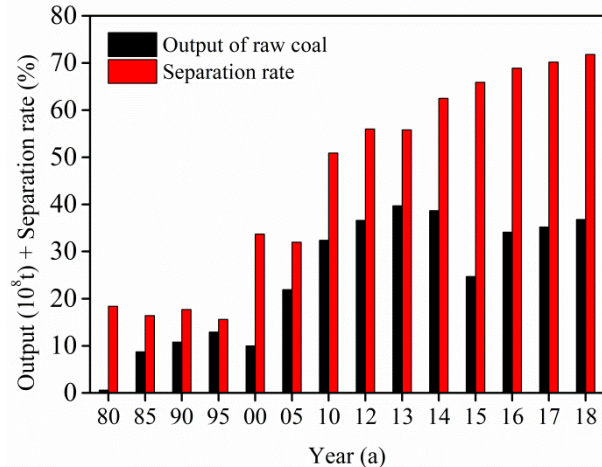


Fig. 1.1. Output and separation rate of raw coal in China

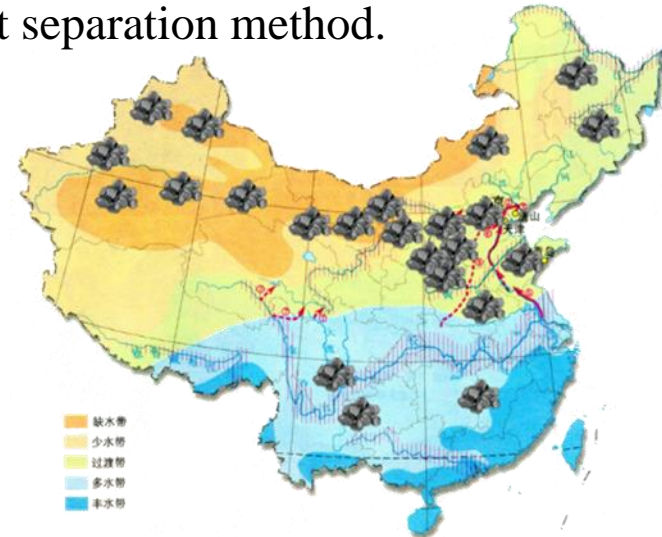


Fig. 1.2. Coal resource distribution in China



➤ Dry Separation Technologies and Parameter Index

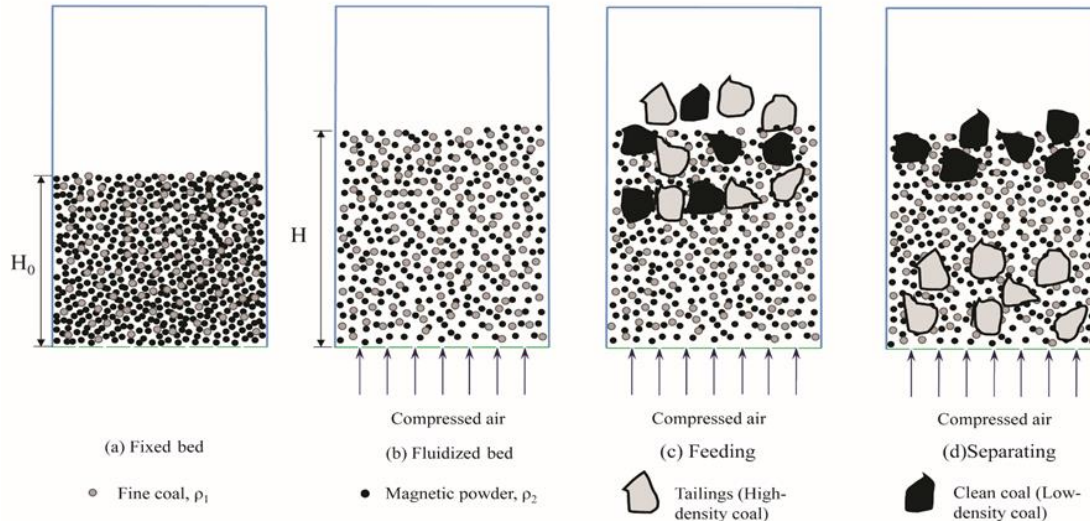
Main Technologies	Feed size/mm	Mineral properties	Possible deviation	Application
Air Dense Medium Fluidized Bed	-50+6	Density	0.05	Industrial scale
Compound Dry Separator	-80	Density	0.2	Industrial scale
Air jigging Separator	-30	Density	0.26	Industrial scale
Vibrating dense medium fluidized bed	-6+1	Density	0.065~0.085	Pilot scale
Vibrating Fluidized Bed with Autogenous Medium	-6+1	Density	0.175~0.225	Laboratory scale
Pulsed Dense-Phase Fluidized Bed	-6+1	Density	0.10~0.19	Laboratory scale
Air Dense Medium Magnetically Fluidized Bed	-6+1	Density	0.068~0.095	Laboratory scale
Countercurrent Separator	-8+1	Density	0.07~0.23	Laboratory scale
TDS Intelligent Dry Separator	-300+25	Luster	-	Industrial scale
Tribo Electrostatic Separator	-0.5	Dielectric property	-	Laboratory scale
Microwave Energy Separator	-0.5	Dielectric property	-	Laboratory scale

Air dense medium fluidized bed has the advantages of **wide feed size** and **high separation accuracy**.



➤ Principle of the Air dense medium gas-solid fluidized bed

- ❑ Magnetic powder (0.074~0.3mm) and fine coal particles (<0.5mm) are used as binary heavy media.
- ❑ Minerals would sink or float based on density stratification.



Experimental

Experimental setup

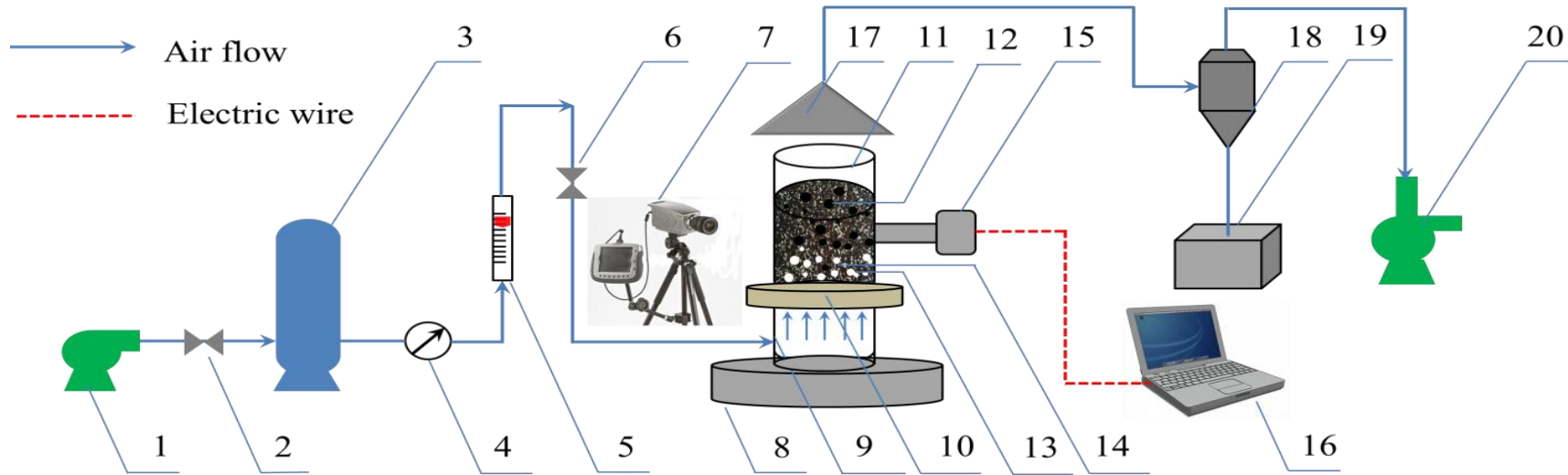


Fig. 2.1 Schematic of the experimental apparatus: 1- Air blower, 2-Butterfly valve I, 3-Air buffer, 4-Pressure meter, 5-Rotameter, 6-Butterfly valve II, 7-High speed camera, 8-Pedestal, 9-Air chamber, 10-Air distributor, 11-Fluidized bed container, 12-Concentrate (clean coal), 13-Binary dense media, 14-Tailing (gangue), 15-Pressure transducer, 16-Signal processing and output device, 17-Dust cover, 18-Dust collector, 19-Dust box, 20-Induced draft fan.



Experimental material

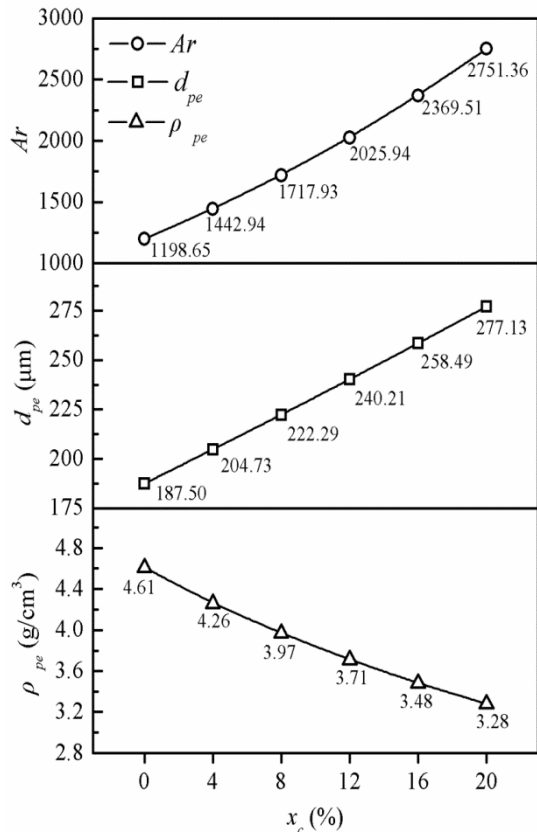


Fig. 2.2 Properties of density, size and Ar of the binary mixture with different x_c

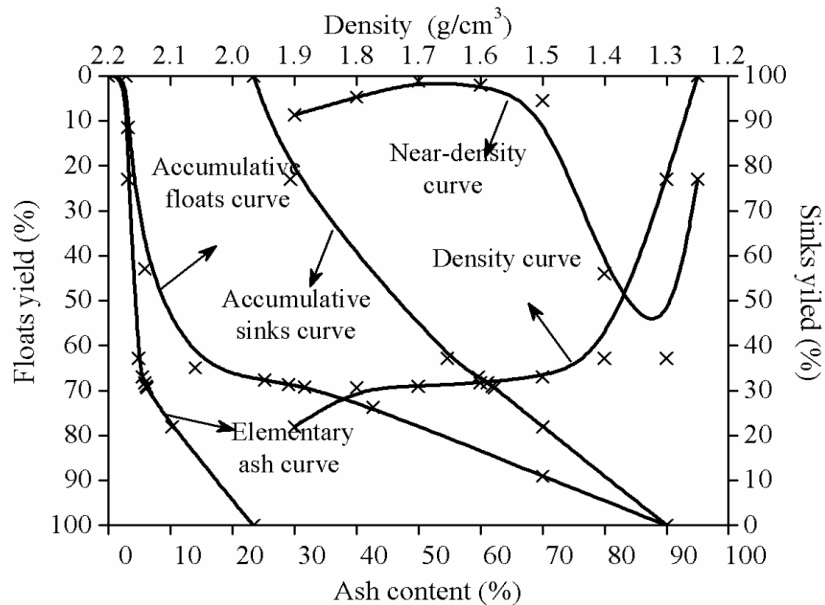


Fig. 2.3 The washability curves of raw coal

- Effect of the increase of d_{pe} was more notable than that of the decrease of ρ_{pe} on the variation of Ar .
- Raw coal samples belonged to a type of **moderate-difficulty** for coal separation.

Results and discussions

► Analysis and fitness of incipient fluidization velocity U_{mf}

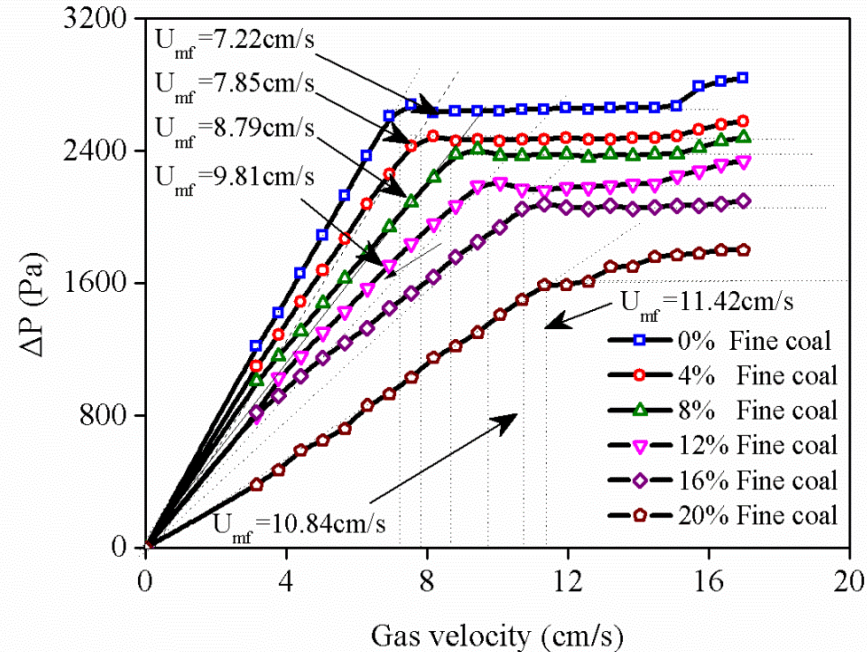


Fig. 3.1. The incipient fluidization velocities for different weight proportions of fine coal

- The incipient fluidization velocity U_{mf} is extremely important because it determines the onset of fluidization and bubbling phenomena in a gas-solid fluidized bed.
- U_{mf} increased from 7.22cm/s to 11.42cm/s with the x_c increasing from 0 to 20%.



➤ Fitness of incipient fluidization velocity U_{mf}

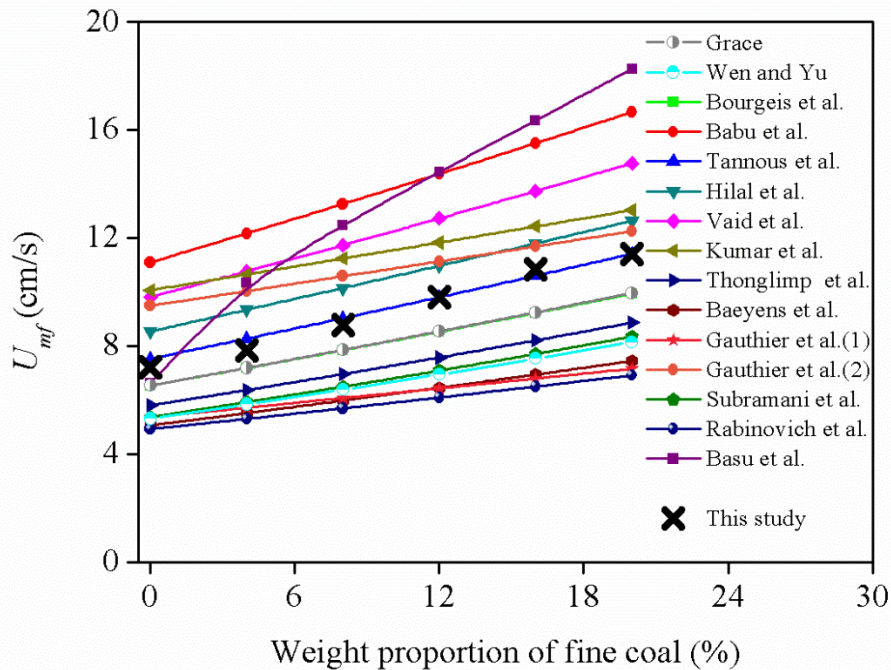


Fig. 3.2. The relationship between U_{mf} and x_c with different empirical correlations

$$U_{mf} = \frac{\mu \left[\left(23.785^2 + 0.0413Ar \right)^{0.5} - 23.785 \right]}{\rho_g \cdot d_{pe}}$$

Different empirical correlations showed the similar variation tendency that U_{mf} gradually increased with x_c .

The relationship between U_{mf} and x_c had a higher fitting degree with the empirical correlation given by *Tannous et al.*

U_{mf} was **more sensitive** to the variation of d_{pe} than that of ρ_{pe} .



Results and discussions

➤ Derivation process of the modified model for predicting bed density

$$G_b = \Psi (U_g - U_{mf}) A \quad \text{Hillgardt et al.}$$

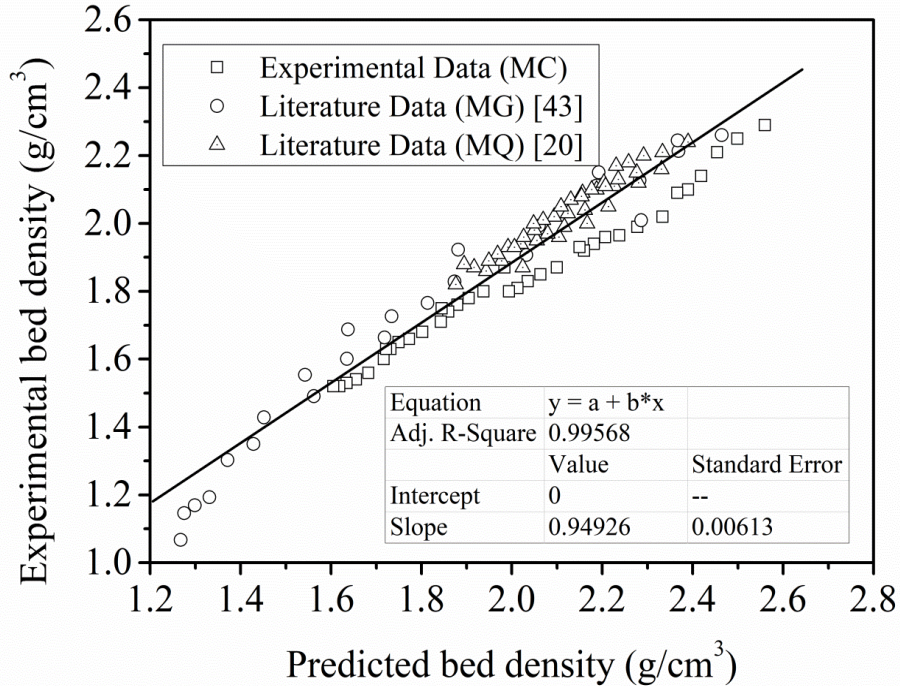
$$\Psi = 1.64 Ar^{-0.2635} \quad \text{Geldart et al.}$$

$$\bar{\rho}_{bed} = (1 - \varepsilon_{mf})(\rho_p - \rho_g) \left(1 - \frac{\Psi}{1 + 1.3(h + 4A_D^{0.5})(U_g - U_{mf})^{-0.8}} \right) + \rho_g \quad \text{Fu et al.}$$

$$\bar{\rho}_{bed} = \rho_p (1 - \varepsilon_{mf}) \left(1 - \frac{1.64 Ar^{-0.2635}}{\frac{1}{H} \cdot \int_0^H [1 + 1.3(h + 4A_D^{0.5})(U_g - U_{mf})^{-0.8}] dh} \right)$$



➤ Linear fitting of predicted bed density with 104 group data



$$\rho_{pre-bed} = 0.94926 \rho_p (1 - \varepsilon_{mf}) \left(1 - \frac{1.64 Ar^{-0.2635}}{1 + 0.65(H + 8A_D^{0.5})(U_g - U_{mf})^{-0.8}} \right)$$

The value of *Adj R-Square* was **0.99568** with the standard error less than 0.01, indicating well-fitting.

Fig. 3.3. Comparison of the calculated bed density and the experimental bed density



➤ Comparison of accuracy using different predicted models

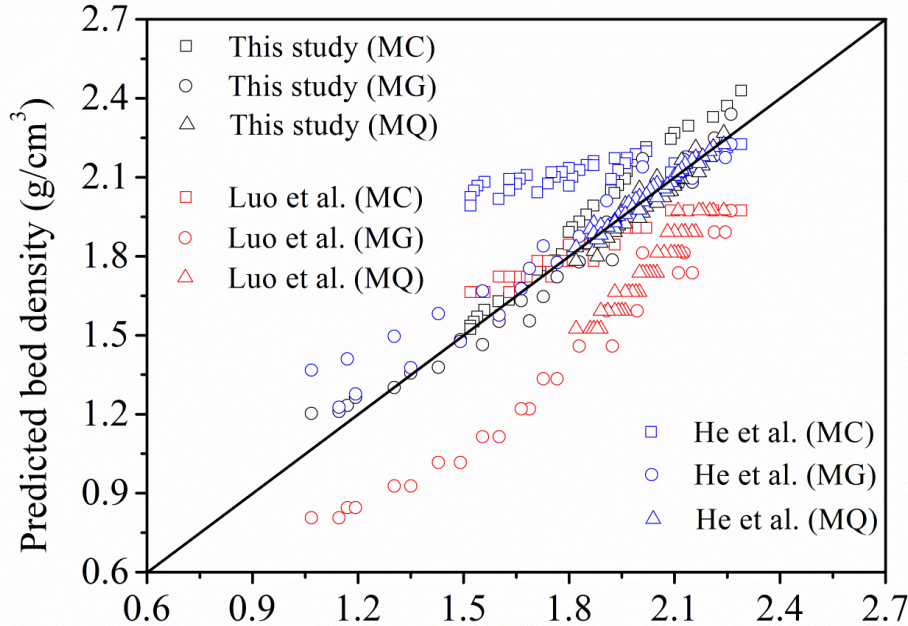


Fig. 3.4. Comparison of the predicted bed density and the experimental bed density with different binary dense media using different predicted models

Source	Calculation correlation	PCCs
Luo et al.	$\rho_{pre-bed} = \frac{1}{0.08 + 1.16e^{-(1-x_c)}}$	0.8170
He et al.	$\rho_{pre-bed} = \frac{\rho_{b1} - 0.904\rho_{b2}\omega}{1.143 + 5.89 \times 10^{-4} e^{N/0.33}}$	0.7823
This Study	$\rho_{pre-bed} = 0.94926\bar{\rho}_{bed}$	0.9679

- He et al. was more suitable for predicting the **higher density**.
- Luo et al. was more applicable for predicting the **lower density**.
- The modified model of this study was applied to predict **wide-density-range**.



➤ Stability and uniformity of bed density

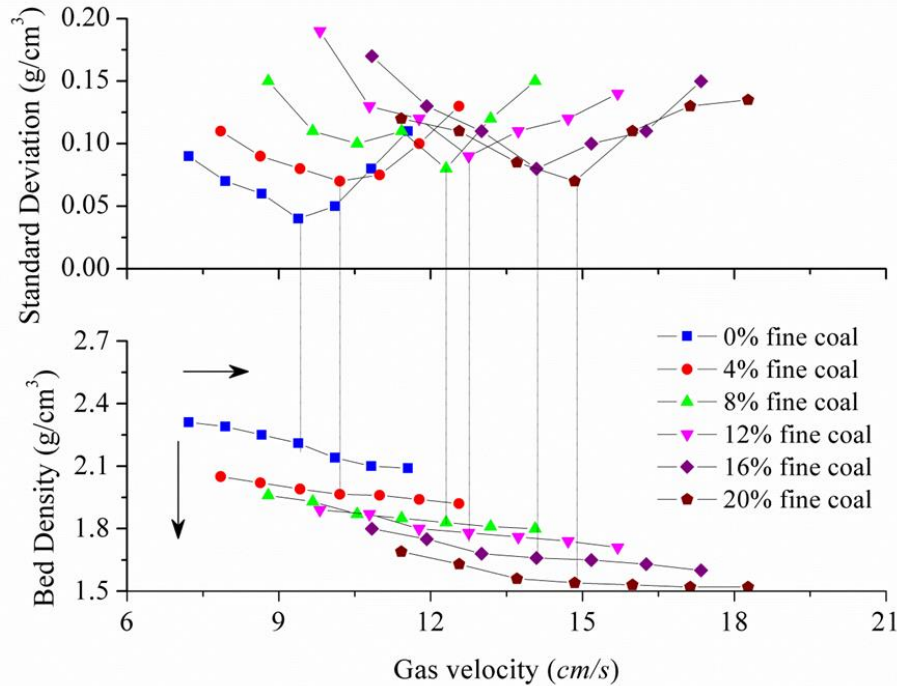


Fig. 3.5. Variations of bed density and S_p with the increase of the gas velocity for various x_c

- The optimal fluidization number were almost 1.3 for various x_c .
- The gas velocity within a suitable range could facilitate the uniform mixing of binary dense media and improve the fluidization quality.
- The ADMGFB using binary dense media could efficiently adjust bed density in a certain variation range.

► Stability and uniformity of bed density

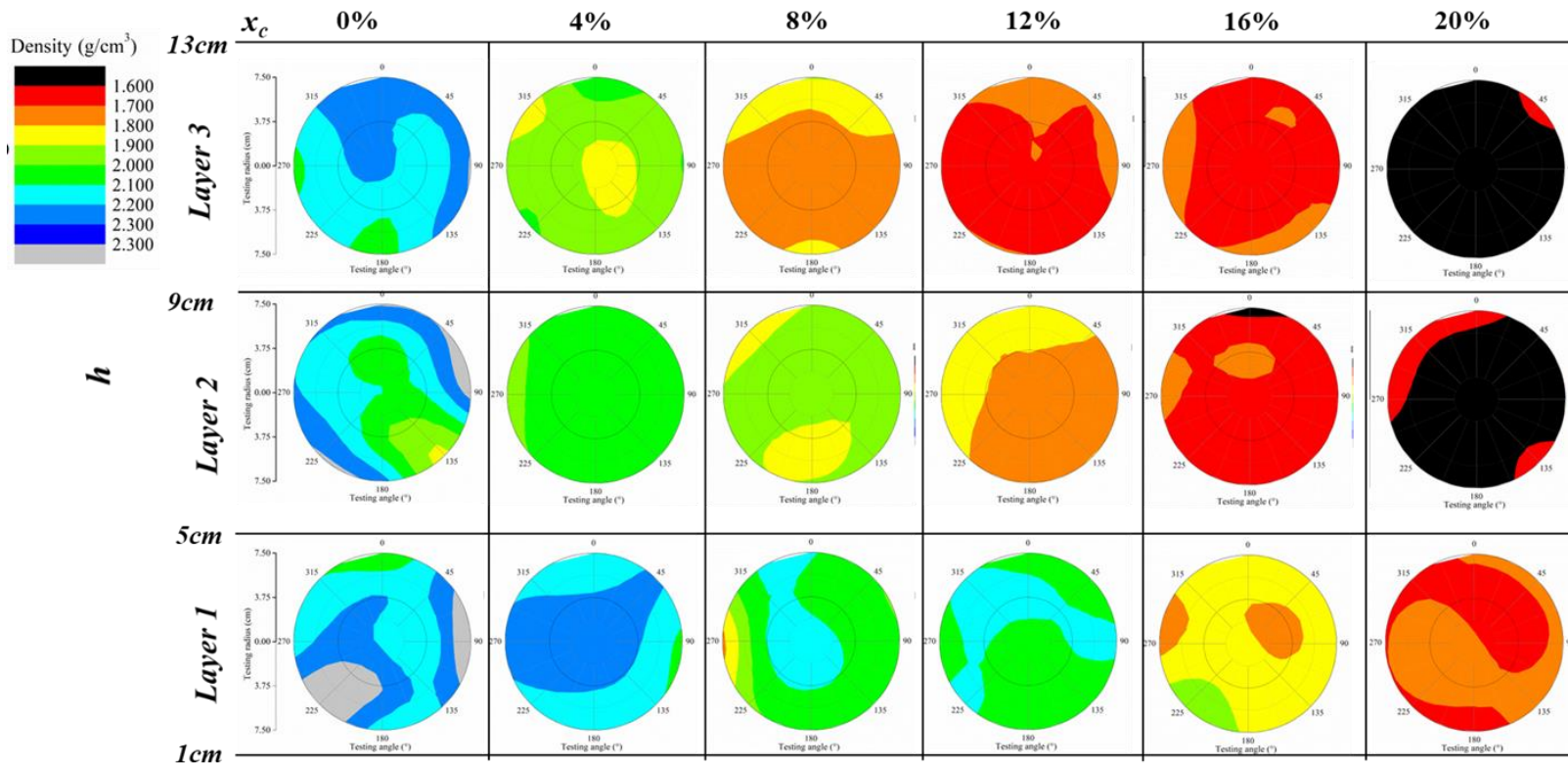
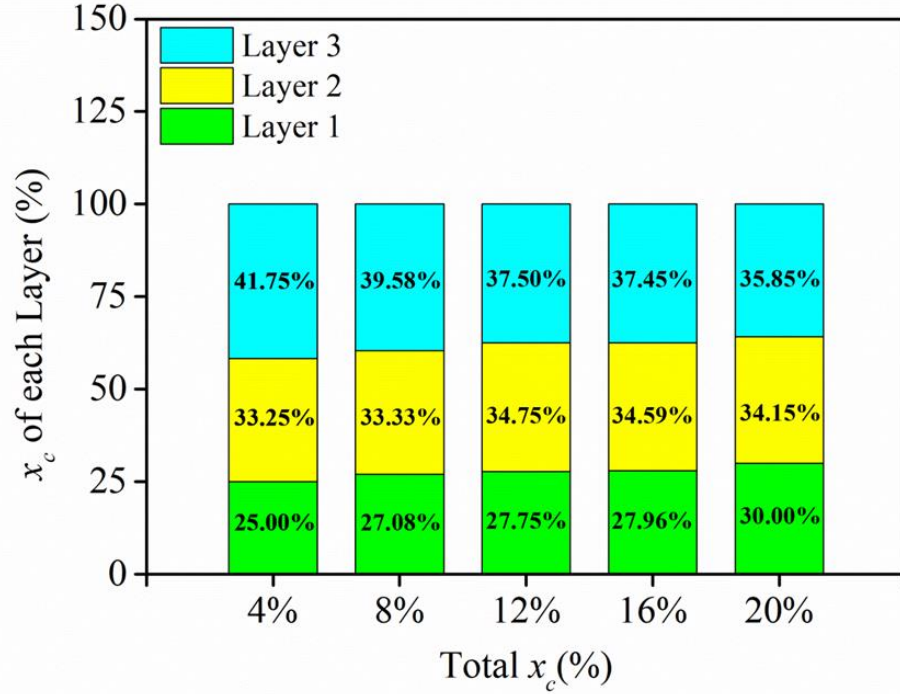


Fig. 3.6. Variation regulation of the density distribution of the bed layer along the radial direction of the bed ($N=1.3$)



➤ Stability and uniformity of bed density



□ The distribution of fine coal of different layers became more uniform with the increase of the total x_c . Therefore, the uniform distribution of binary dense media facilitated the uniformity of fluidization.

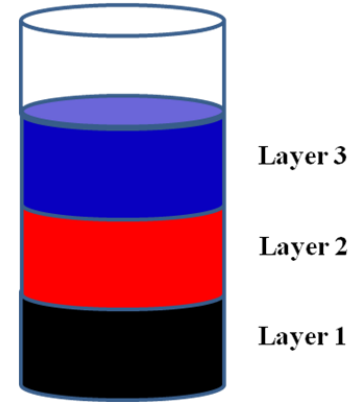


Fig. 3.7. Distribution of fine coal of different layers with different total x_c



➤ Separation performance of ADMGFB under suitable conditions

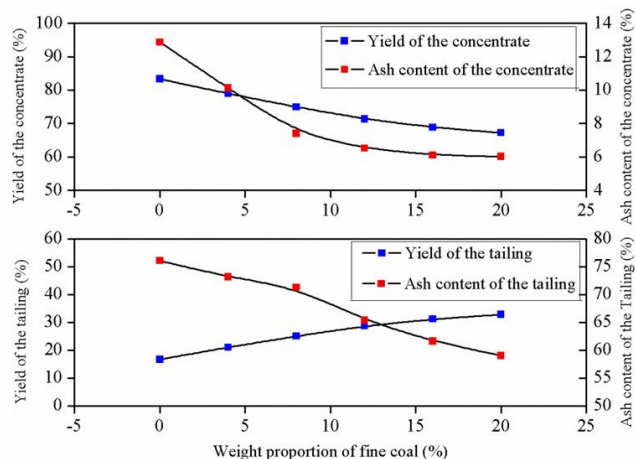


Fig. 3.8. Yield and ash content of clean coal and tailing with different weight proportions of fine coal

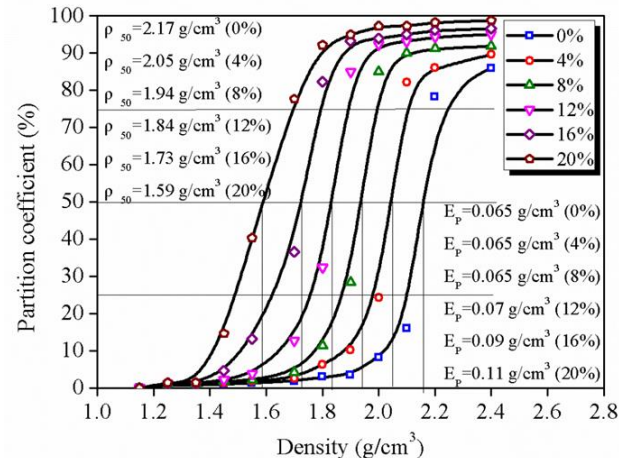


Fig. 3.9. Partition curves of separation experiments with different weight proportions of fine coal

- The satisfactory yield and ash content of clean coal with the optimum probable error E value indicated the separation performance of coal was notably intensified in ADMGFB using binary dense media.



Conclusion

- ❑ The correlation model of U_{mf} and x_c could be used to predicted the incipient fluidized velocity of binary dense media in ADMGFB.
- ❑ A modified model to predict bed density in ADMGFB with binary dense media was proposed based on the two-phase fluidization theory.
- ❑ The binary dense media could efficiently facilitate the uniformity of fluidization and the stability of bed density with the fluidization number of 1.3.
- ❑ The separation performance of coal was notably intensified in ADMGFB using binary dense media.

- The authors are grateful to the financial support by National Science and Engineering Research Council of Canada, and National Natural Science Foundation of China (No. 51620105001).
- Thank to the My supervisor Prof. **Yuemin ZHAO**, and the Mineral Processing Engineering Center of CUMT.

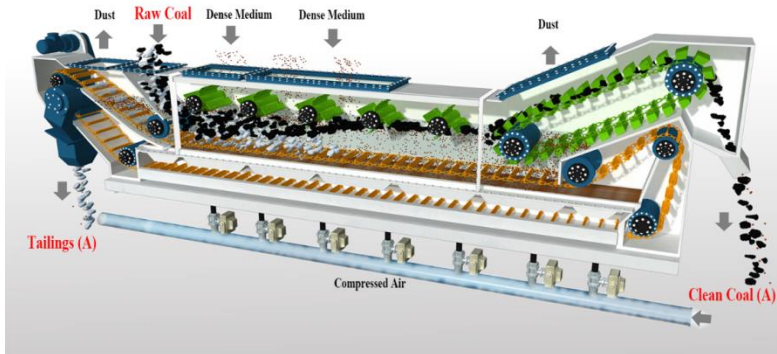


Fig. 3.10. Continuous Industrial Separator



Fig. 3.11. Modular Air Dense Medium Fluidized Bed Industrial Separator



Thank you for your attention!

Presented by Chengguo LIU

MAY 28, 2019

Room: Nanning Room No.1

Guilin Shangri-La Hotel | Guilin, China